PNAS RESEARCH ARTICLE | CHEMISTRY

# Preparation of methanediamine ($CH_2(NH_2)_2$)—A precursor to nucleobases in the interstellar medium

Joshua H. Marks[a,b], Jia Wang[a,b], Ryan C. Fortenberry[c,1], and Ralf I. Kaiser[a,b,1]

Edited by Robert Field, Massachusetts Institute of Technology, Cambridge, MA; received October 10, 2022; accepted November 5, 2022

**Although methanediamine ($CH_2(NH_2)_2$) has historically been the subject of theoretical scrutiny, it has never been isolated to date. Here, we report the preparation of methanediamine ($CH_2(NH_2)_2$)—the simplest diamine. Low-temperature interstellar analog ices composed of ammonia and methylamine were exposed to energetic electrons which act as proxies for secondary electrons produced in the track of galactic cosmic rays. These experimental conditions, which simulate the conditions within cold molecular clouds, result in radical formation and initiate aminomethyl ($\dot{C}H_2NH_2$) and amino ($NH_2$) radical chemistry. Exploiting tunable photoionization reflectron time-of-flight mass spectrometry (PI-ReToF-MS) to make isomer-specific assignments, methanediamine was identified in the gas phase upon sublimation, while its isomer methylhydrazine ($CH_3NHNH_2$) was not observed. The molecular formula was confirmed to be $CH_6N_2$ through the use of isotopically labeled reactants. Methanediamine is the simplest molecule to contain the NCN moiety and could be a vital intermediate in the abiotic formation of heterocyclic and aromatic systems such as nucleobases, which all contain the NCN moiety.**

interstellar ice | astrochemistry | ionization potentials | radical reactions | reaction mechanism

## Significance

Methanediamine ($CH_2(NH_2)_2$) represents a target of computational study, and while its dihydrochloride salt is used in synthetic preparations, the free diamine exists only as a transient in solution. Here, we prepare and identify methanediamine via energetic processing of low-temperature ices followed by sublimation into the gas phase. This finding shows that interstellar ices subjected to ionizing radiation, such as galactic cosmic rays and ultraviolet light, exhibit unique chemistry in which highly unstable species are produced and preserved. Both ammonia and methane are abundant in interstellar ices where radical reactions can readily produce methanediamine. Its subsequent sublimation into the gas phase in star-forming regions indicates that this species is a candidate for detection by radio telescopes.

Nitrogen represents a central element in contemporary biomolecules such as in amino sugars, amino acids, and nucleobases (1). Nitrogen is also incorporated into nearly one-third of some 300 molecules identified in the interstellar medium (ISM) and around circumstellar envelopes (2). However, most nitrogen-containing molecules in deep space carry exclusively nitrile moieties (RC≡N) which are weakly electrophilic in contrast to nucleophilic amines (RNR'R"), imines (R=NR'), and amides (RCONHR') needed for life as we know it (2–4). So far, only two closed-shell molecules have been detected astronomically which contain more than one nitrogen-carrying moiety other than nitrile: urea ($CO(NH_2)_2$) (5, 6) and carbodiimide (HN=C=NH) (7). An understanding of the origin and fundamental chemistry of the NCN moiety in deep space is central to the RNA world hypothesis for the origin of life (8–10) because all nucleobases found in contemporary RNA and DNA contain this very NCN moiety (Scheme 1). Here, the abiotic synthesis and gas-phase detection of methanediamine (**1**, $CH_2(NH_2)_2$) are reported as a prototype system for unraveling the origin and incorporation of the NCN moiety into complex organic molecules of potential astrobiological importance.

The bulk of prior scholarship has employed methanediamine (**1**) as a model compound to study systems containing the R–X–C–Y backbone, where X has a lone pair and Y represents any element more electronegative than carbon such as R–$NHCH_2NH_2$. Molecules carrying this moiety reveal a preference for the gauche configuration resulting from internal rotation along both the X–C and C–Y bonds in what is known as the generalized anomeric effect (11–19). Negative hyperconjugation, where electron density is donated from the non-bonding pair of nitrogen to the CH antibonding ($\sigma^*$) orbital, contributes to this effect and has a particularly strong influence on the conformational structure of methanediamine (**1**) (11, 13, 14, 16). Since the donation increases antibonding character, this tends to weaken the carbon–hydrogen bonds while stabilizing radicals formed by elimination of atomic hydrogen from carbon (11, 20–23). Substitution of two hydrogen atoms in methane ($CH_4$) with the amino group (-$NH_2$) stabilizes the diaminomethyl radical ($\dot{C}H(NH_2)_2$) by 43 kJ $mol^{-1}$ which allows for unusual radical reactions like [1] to occur more readily (Scheme 2) (20, 23). The amines also stabilize the singlet state of diaminocarbene ($\overline{C}(NH_2)_2$) by 202 kJ $mol^{-1}$ while increasing the energy of the triplet ($C(NH_2)_2$) by 65 kJ $mol^{-1}$; this results in a singlet ground state which can participate in recombination [2] or spin-allowed carbene insertion [3] (24).

Unlike methanediamine (**1**), the hydrochloride salt of methanediamine has been employed in organic preparative solution chemistry as a reactant for more than a century (25). Upon neutralization of the salt, methanediamine (**1**) is presumed to exist as a highly

Author contributions: J.H.M. and R.I.K. designed research; J.H.M., J.W., and R.C.F. performed research; J.H.M. analyzed data; J.H.M. and R.I.K. wrote the paper; R.C.F. performed calculations.

The authors declare no competing interest.

This article is a PNAS Direct Submission.

Copyright © 2022 the Author(s). Published by PNAS. This article is distributed under Creative Commons Attribution-NonCommercial-NoDerivatives License 4.0 (CC BY-NC-ND).

[1]To whom correspondence may be addressed. Email: r410@olemiss.edu or ralfk@hawaii.edu.

This article contains supporting information online at https://www.pnas.org/lookup/suppl/doi:10.1073/pnas.2217329119/-/DCSupplemental.

Published December 12, 2022.

Downloaded from https://www.pnas.org by University of Hawaii at Manoa Library on December 12, 2022 from IP address 128.171.57.189.

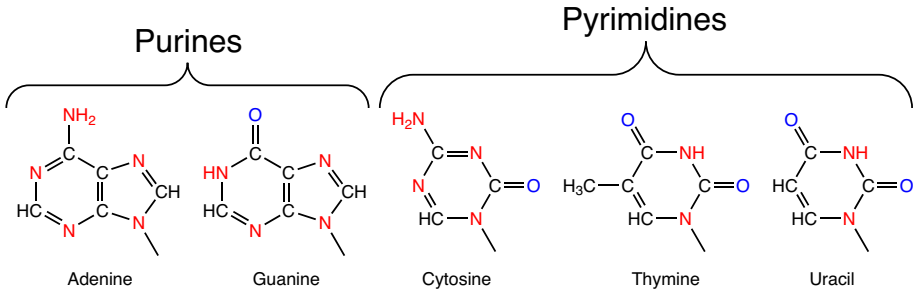


**Scheme 1.** Nucleotides found in RNA and DNA, all of which contain the NCN moiety exhibited by methanediamine (1, $CH_2(NH_2)_2$).

reactive intermediate. The nucleophilic nature of amines allows this transient to participate in substitution reactions [4]–[8] (26–29). This can take the form of substitution for an alcohol or ether in [4] (26) or substitution of an aldehyde (RCHO) or ketone (RC(O)R') via [5] by an imine (29) or a diazaspirane, respectively (30). Its bifunctional nature allows for participation in ring-closure reactions accompanied by aromatization as demonstrated in [6] (27) and [7] (28); these show that both amine and imine bonds can form resulting in nitrogen-substituted polycyclic aromatic hydrocarbons (28). The potential formation of aromatic heterocycles from methanediamine (**1**) via nucleophilic chemistry may provide a route to the abiotic formation of nucleobases in the ISM. Pyrimidine (*c*-NCHNCHCHCH) forms the core structure of cytosine, thymine, and uracil (Scheme 1). Given the recent observation of 3-hydroxypropenal (OCHCHCHOH) toward the protostar IRAS 16293-2422 (28), nucleophilic substitution with methanediamine (**1**) in reaction [8] may provide a facile route to the abiotic formation of pyrimidine via $S_N2$ nucleophilic substitution of amines onto aldehydes which has been demonstrated to operate in low-temperature acidic ices (31, 32).

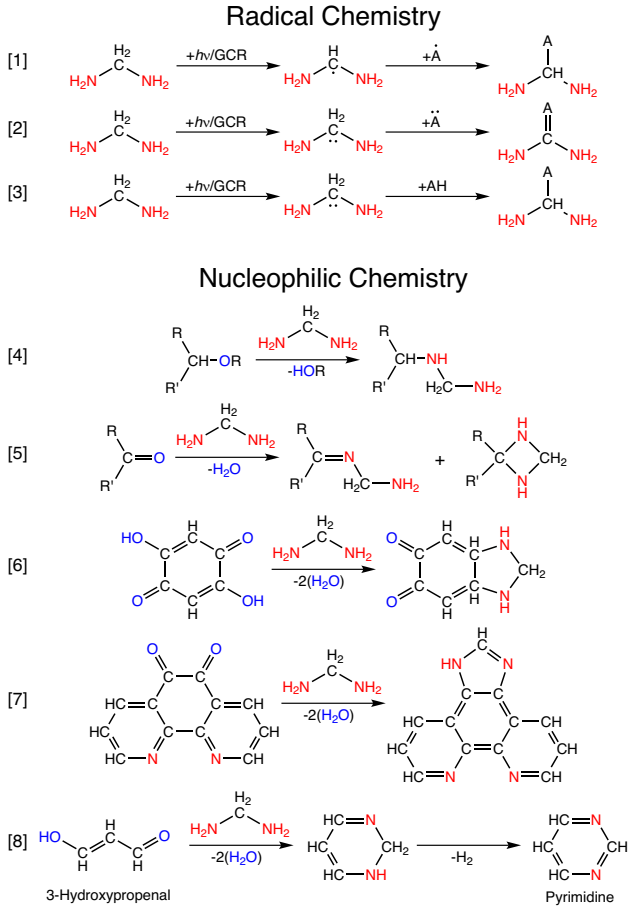


**Scheme 2.** Representative reactions of methanediamine ($CH_2(NH_2)_2$) including radical–radical recombination [1]–[3] initiated by energetic photons (h$\nu$) or GCRs and nucleophilic substitution [4]–[8].

Here, by exploiting isomer-selective photoionization combined with reflectron time-of-flight mass spectrometry (PI-ReToF-MS), the preparation and gas-phase detection of methanediamine (**1**) is reported. Interstellar analog ices of methylamine ($CH_3NH_2$) and ammonia ($NH_3$) were exposed to proxies of galactic cosmic rays (GCRs) in the form of energetic electrons. Reactions which may form both methanediamine (**1**, $CH_2(NH_2)_2$) and methylhydrazine (**2**, $CH_3NHNH_2$) in this simulated interstellar environment were investigated (Fig. 1). Isotopic substitution experiments along with tunable vacuum ultraviolet light (VUV) photoionization at discrete energies reveal unambiguously the selective preparation of methanediamine (**1**) via a carbon–nitrogen bond coupling through the radical–radical reaction of aminomethyl (**A**, $\dot{C}H_2NH_2$) and amino (**C**, $NH_2$) radicals thus providing a facile to the previously elusive methanediamine (**1**).

## Results

PI-ReToF-MS data collected in these experiments are shown as a function of temperature in Fig. 2. In these experiments, single-photon ionization with VUV laser light is employed to ionize molecules as they sublime from the ice after the exposure to GCR proxies (*SI Appendix*). This is a fragmentation-free or "soft" ionization method, particularly in comparison with electron impact ionization. By using tunable VUV light, the photon energy can be selected to selectively ionize and hence to discriminate isomers with different ionization energy as molecules cannot be ionized when the photon energy is less than their adiabatic ionization energy. Furthermore, isotopic labeling was used to verify the molecular formula, and in some cases the formation mechanism, of observed molecules. By exploiting these techniques, PI-ReToF-MS experiments separate molecules by mass, sublimation temperature, and ionization energy to confidently assign the identity of reaction products in the analog ice: methanediamine (**1**).

The adiabatic ionization energy is unknown for methanediamine (**1**) and has been measured with substantial error for methylhydrazine (**2**) (33). Therefore, adiabatic ionization energies were computed for all possible conformers of both methanediamine (**1**) and methylhydrazine (**2**) with high-quality CCSD(T) complete basis set computations expected to have a maximum error of ±0.05 eV (*SI Appendix*, Table S1) (34). Accounting for all conformers, the range of adiabatic ionization energies of methanediamine (1) is 8.54–8.75 eV and 7.44–7.67 eV for methylhydrazine (**2**). Photoionization with 9.20 eV photons is therefore capable of ionizing both of these molecules, while 8.00 eV photons can only ionize methylhydrazine (**2**). Collected ion counts at a

Downloaded from https://www.pnas.org by University of Hawaii at Manoa Library on December 12, 2022 from IP address 128.171.57.189.

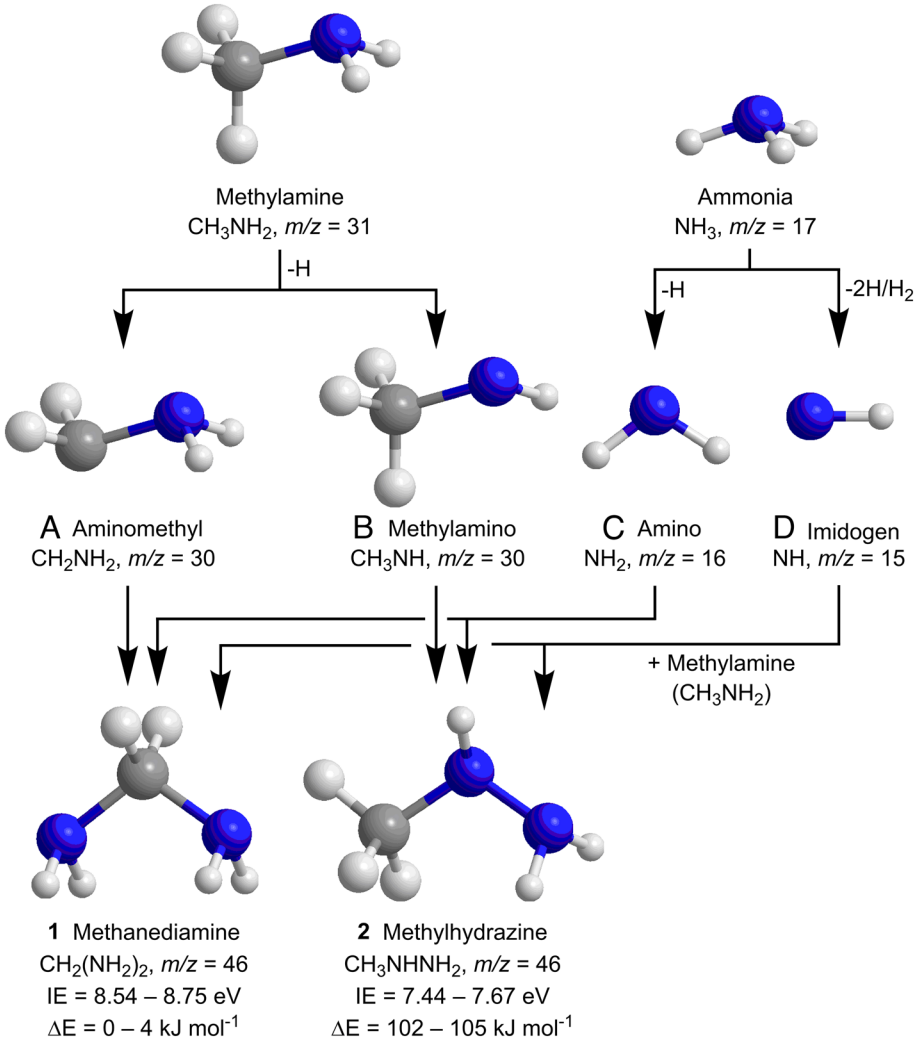


**Fig. 1.** Reaction scheme for radical reactions of ammonia ($NH_3$) and methylamine ($CH_3NH_2$) to form methanediamine (**1**, $CH_2(NH_2)_2$) and methylhydrazine (**2**, $CH_3NHNH_2$) via radical–radical recombination or insertion of imidogen into methylamine. Computed relative (ΔE) and adiabatic ionization energies (IE) are presented as ranges that include all conformers.

mass-to-charge ratio (*m/z*) = 46 ($CH_6N_2$) are reported as a function of temperature in Fig. 3*A*. Photoionization at 9.20 eV produced a small peak at 120 K and a larger sublimation event at 152 K. Neither of these events is observed at 8.00 eV. This reveals that the molecule(s) responsible for these peaks must have an adiabatic ionization energy between 8.00 and 9.20 eV. Since we can eliminate the possibility of the presence of methylhydrazine (**2**), this peak must therefore be linked to methanediamine (**1**).

To provide further evidence in the observation of this molecule, isotopic substitution experiments were carried out to ensure that the observed compound does, in fact, have the molecular formula ($CH_6N_2$). In detail, isotopically labeled ammonia and methylamine were used to verify the formula of the ions detected in Fig. 3*A*. The smaller peak at 120 K occurs at the same temperature as a major peak found at *m/z* = 45; this sublimation event is connected to dimethylamine which is present as a trace contaminant in the methylamine sample and observed here as the naturally occurring dimethylamine-$^{13}$C. If it is assumed that carbon can make up to four bonds, nitrogen three, and hydrogen one, then the only possible molecular formulas for *m/z* = 46 are $H_4N_3$ and $CH_6N_2$. When $^{15}$N-ammonia–methylamine ice was examined, the peak at 152 K and *m/z* = 46 was (Fig. 3*A*) found to shift to *m/z* = 47 (Fig. 3*B*). From this isotopic shift, it is concluded that there must be at least one nitrogen present in the observed molecule which must originate in the ammonia component of the ice. Furthermore, this is in agreement with the reaction shown in Fig. 1 which demonstrates the incorporation of one nitrogen from ammonia via the amino radical (**C**, $NH_2$). When ammonia-$d_3$–methylamine-$d_5$ ice was examined, the peak at 152 K was found to shift from *m/z* = 46 to 52 (Fig. 3*C*). This can only happen if the molecule being ionized contains six or more hydrogen atoms, which excludes the possibility that $H_4N_3$ is being observed and confirms that the correct molecular formula is $CH_6N_2$. It was also noted that the peak of the temperature programmed desorption (TPD) profiles observed in this deuterated ice shifts from 152 K to 160 K. This is likely due to an increase of molecular weight by 6 amu resulting in an elevated sublimation temperature (35).

## Discussion

Since the ionization energy and the molecular formula match only those of methanediamine (**1**), this constitutes the conclusive observation of this molecule. No signal is observed at *m/z* = 46 with a photon energy of 8.00 eV. Therefore, if methylhydrazine (**2**, IE = 7.44–7.67 eV) is produced, it is not present in detectable quantities. If the reaction proceeds by radical–radical recombination, this would suggest a lack of formation of the methylamino radical (**B**, $CH_3NH$). Prior experiments, in which pure methylamine ice was irradiated under similar conditions as the present experiment, did not observe reaction products from recombination of the methylamino radical, i.e., 1,2-dimethylhydrazine ($CH_3NHNHCH_3$) or *N*-methylmethanediamine ($CH_3NHCH_2NH_2$) (36). The only

Downloaded from https://www.pnas.org by University of Hawaii at Manoa Library on December 12, 2022 from IP address 128.171.57.189.

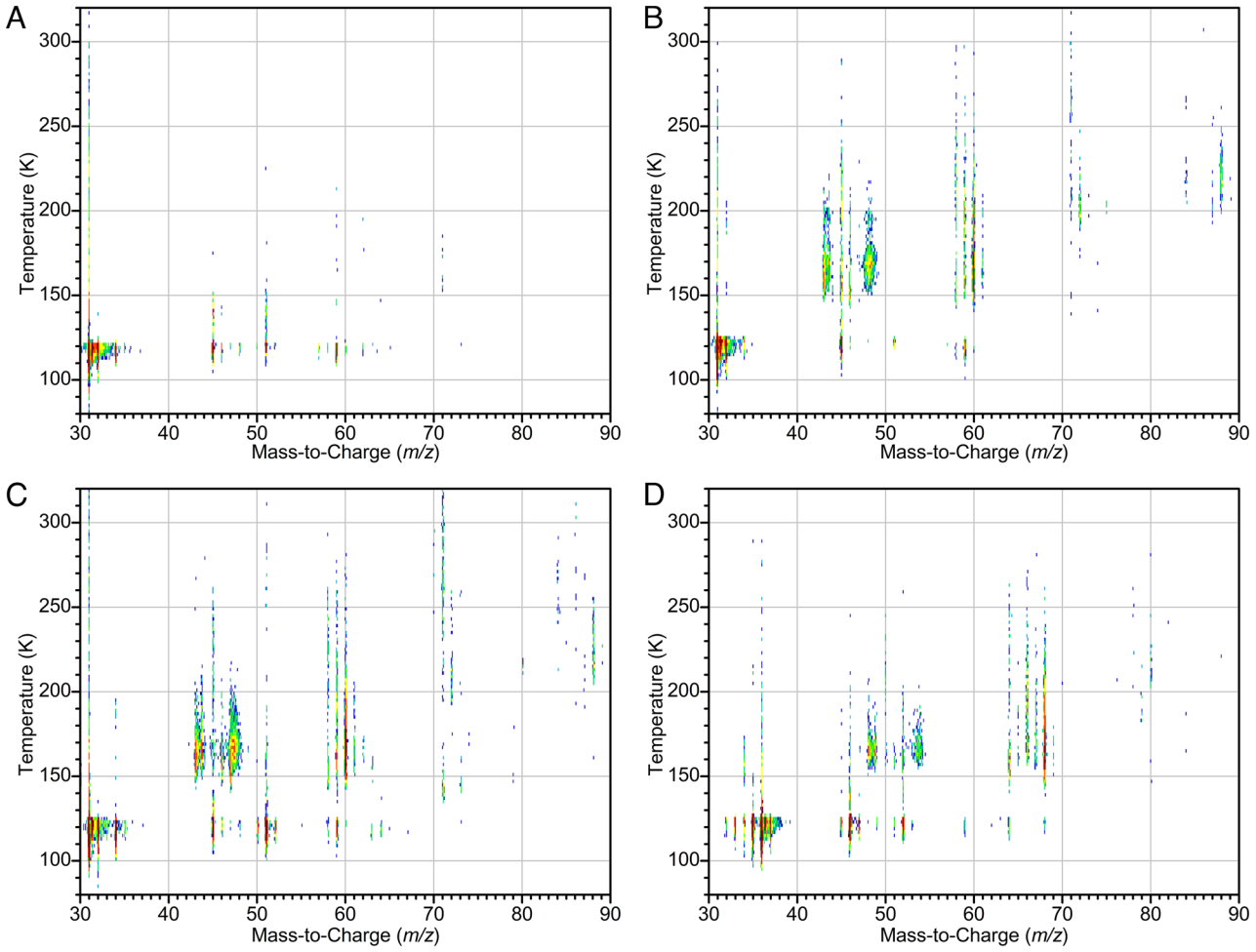


**Fig. 2.** Photoionization reflectron time-of-flight (PI-ReToF) mass spectra measured during TPD plotted as a function of temperature. Experiments were conducted with (*A*) ammonia–methylamine ice without irradiation, and with irradiation of 0.21 ± 0.02 eV molecule$^{-1}$ for ammonia and 0.38 ± 0.04 eV molecule$^{-1}$ for methylamine in (*B*) ammonia–methylamine ices, (*C*) $^{15}$N-ammonia–methylamine ice, and (*D*) ammonia-$d_3$–methylamine-$d_5$ ice.

reaction product identified was ethylenediamine ($NH_2CH_2CH_2NH_2$), which originates from radical–radical recombination of aminomethyl radicals (**B**, $\dot{C}H_2NH_2$) (36). Since solely reaction products from aminomethyl (**B**) have been observed in pure methylamine and mixed ammonia–methylamine ices, the reaction mechanism responsible likely proceeds by radical–radical recombination (Fig. 1).

The process to form methanediamine (**1**) via radical–radical reaction [9] is endoergic by 488 ± 3 kJ mol$^{-1}$; this energy can be imparted by the impinging electrons. The distance between the ice surface and the ionization region of 2.0 ± 0.5 mm along with the range of sublimation temperatures implies that methanediamine (**1**) has to "live" at least an average of 7.6 ± 1.9 μs. However, lifetimes of the ions must be at least 26.88 ± 0.07 μs to be detected. Note that the "thermal" decomposition of methanediamine (**1**) to methanimine ($H_2CNH$) plus ammonia ($NH_3$) [10] is calculated to be endoergic by 46 ± 3 kJ mol$^{-1}$, also supporting its gas-phase stability.

$$CH_3NH_2 + NH_3 \rightarrow CH_2(NH_2)_2 + 2H \quad \textbf{[9]}$$

$$CH_2(NH_2)_2 \rightarrow H_2CNH + NH_3 \quad \textbf{[10]}$$

Previous experimental investigations in ices have shown that isoelectronic molecules methanediol (37) ($CH_2(OH)_2$) and aminomethanol (38) ($NH_2CH_2OH$) form in irradiated ices and survive into the gas phase and upon photoionization. The minimum energy conformers (Scheme 3) (37, 38) of these molecules demonstrate significant variation in bond angles. Methanediamine (**1**) exhibits an NCN angle of 119.0°, while the NCO angle in aminomethanol is the smallest at 110.6°. Both of which are larger than the ideal 109.5° tetrahedral angle for the central carbon atom. Such behavior indicates that electrostatic repulsion from the non-bonding electron pairs along with steric repulsion is present in all three molecules but is more significant for the $NH_2$ than for the OH moiety. While the CH, NH, and OH bond lengths vary little between these molecules, in aminomethanol the C–N single bond is 3 pm shorter, but the C–O bond is 3 pm longer compared to methanediamine (**1**) and methanediol. These variations in bond lengths are likely the result of enhanced transfer of electron density from –$NH_2$ to –OH in aminomethanol upon increasing electronegativity from nitrogen to oxygen. The calculations employed here improve on prior efforts (11, 13, 14) to study methanediamine (**1**) computationally. While the gauche configuration was previously expected to be more stable, higher-level ab initio calculations employed herein indicate the trans configuration across both C–N bonds to be most stable. The discrepancy in relative energies between calculations reported here and prior studies demonstrate the need for the testing and further development of computational methods. The existence of the previously "hypothetical" molecules in Scheme 3 reveals an opportunity for future experimental measurements and detection utilizing the PI-ReToF-MS approach which would aid

Downloaded from https://www.pnas.org by University of Hawaii at Manoa Library on December 12, 2022 from IP address 128.171.57.189.

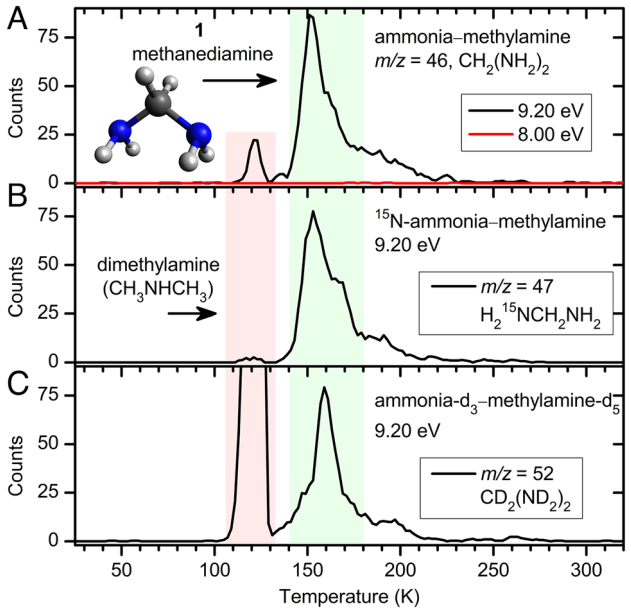


**Fig. 3.** TPD profiles measured during photoionization reflectron time-of-flight (PI-ReToF) mass spectra measurement of ammonia–methylamine ices. Ices formed with natural isotopic abundance (*A*) were examined with photon energy of 9.20 and 8.00 eV and at 9.20 eV with isotopic labeled ices (*B*) $^{15}$N-ammonia–methylamine, and (C) ammonia-$d_3$–methylamine-$d_5$.

in benchmarking the accuracy of quantum chemical calculations and contribute to the development of more accurate and predictive quantum chemical methods.

## Conclusion

These experiments revealed that methanediamine (**1**) can be produced in interstellar ices and is able to sublime intact not only in the laboratory but also in star-forming regions such as Sagittarius B2 (Sgr B2) where its signal may be explored by radio telescopes. Rotational spectroscopy of methanediamine (**1**) in the millimeter and sub-millimeter wave regions would be necessary for the identification of this previously elusive molecule in deep space and should be pursued, and dipole moments are reported in *SI Appendix*, Table S1 to aid in this search. Of the necessary reactants, ammonia is abundant in interstellar ices at fractions of regularly above 15% relative to water as determined in, e.g., the c2d Spitzer survey (39). Methylamine has been detected in the gas phase toward the Sgr B2(N) molecular cloud on the order of $10^{-7}$ relative to molecular hydrogen (40, 41). While much less abundant than ammonia, methylamine has been shown to form in ices from ammonia and methane (42), and methane is nearly as prevalent as ammonia in interstellar ices being found with abundances of up to 13% observed toward EC 92 (43). Therefore, the synthesis and sublimation of methanediamine (**1**) reported here along with the prior detection in interstellar space of its precursors indicate that its preparation in interstellar ices is plausible with ring-closure reactions (Scheme 2) suggesting that methanediamine (**1**) can play a vital role in the abiotic formation of heterocycles and nucleobases in particular.

## Methods and Materials

**Experimental.** All experiments were carried out at the W. M. Keck Research Laboratory in Astrochemistry (44–46). The apparatus consists of a hydrocarbon-free stainless steel ultra-high vacuum chamber with pressures maintained at a few $10^{-11}$ Torr (47). A closed cycle helium refrigerator (Sumitomo Heavy Industries, RDK-415E) is used to maintain a polished silver wafer (12.6 × 15.1 mm) at 5.0 ± 0.2 K. Ices were prepared by passing ammonia (ammonia, Matheson, 99.99%; $^{15}$N-ammonia, Sigma-Aldrich, 98% $^{15}$N; ammonia-$d_3$, Sigma-Aldrich, 99% D) at a partial pressure of 1 × $10^{-8}$ Torr and methylamine (methylamine, 99.5% Matheson TriGas; methylamine-$d_5$, Cambridge Isotope Laboratories, 98% D) at a partial pressure of 1.5 × $10^{-8}$ through separate 10 mm diameter glass capillary arrays. Prior to deposition of deuterated gases, all tubing was filled with deuterated water vapor ($D_2O$) which was also flowed through the capillary arrays to prevent isotope exchange from reducing % D purity. The ice thickness was determined to be 720 ± 30 nm by monitoring the ice deposition with a helium–neon laser (CVI Melles-Griot, 25-LHP-230, 632.8 nm) at a 4° angle of incidence and measuring variations in reflected power due to thin film interference by the ice (48). Ice index of refraction was approximated to be $1.35_5$ by the average of the indexes of refraction of the two components, 1.33 for ammonia and 1.38 for methylamine in amorphous ices at 18 K (49). Fourier transform infrared (FTIR) spectra (Thermo Electron, Nicolet 6700) were measured in the range 6000 to 500 $cm^{-1}$ after ice deposition at 5.0 ± 0.2 K and used to calculate the relative abundance of the two components (*SI Appendix*, Figs. S1–S3 and Table S2). Relative concentrations of ammonia and methylamine in ices (*SI Appendix*, Table S3) were determined using integrated infrared absorptions of $\nu_2$ of ammonia (1070 $cm^{-1}$, 2.1 × $10^{-17}$ cm $molecule^{-1}$) and $\nu_6$ (1420 $cm^{-1}$, 1.8 × $10^{-19}$ cm $molecule^{-1}$), combined $\nu_5$ and $\nu_{12}$ (1433 to 1520 $cm^{-1}$, 1.73 × $10^{-18}$ cm $molecule^{-1}$), and the CH stretching region with $\nu_3$, $\nu_2$, and $\nu_{11}$ (2727 to 3015 $cm^{-1}$, 2.3 × $10^{-17}$ cm $molecule^{-1}$) for methylamine (49, 50).

After deposition, ices were irradiated with 5 keV electrons (SPECS, EQ PU-22) with electron currents and times as listed in *SI Appendix*, Table S3 over an area 160 $mm^2$ at a 70° angle of incidence for an effective dose of 0.20 ± 0.02 eV $molecule^{-1}$ for

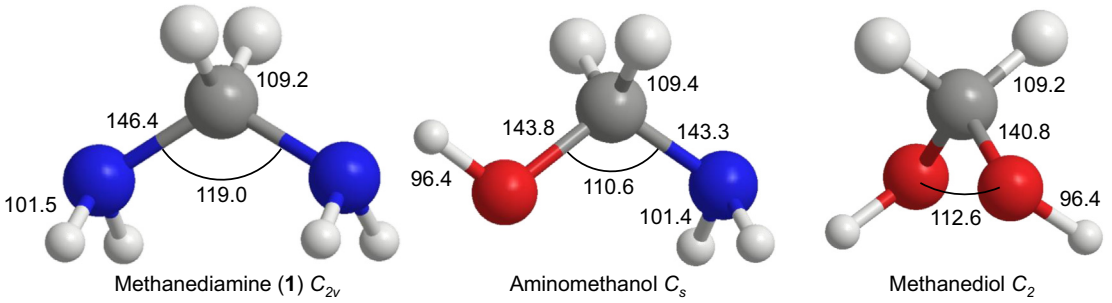


**Scheme 3.** CCSD(T)/aug-cc-pVTZ optimized structures of methanediamine (1, $CH_2(NH_2)_2$), methanolamine ($H_2NCH_2OH$), and methanediol ($CH_2(OH)_2$) with bond lengths (pm) and selected angles (degrees).

Downloaded from https://www.pnas.org by University of Hawaii at Manoa Library on December 12, 2022 from IP address 128.171.57.189.

ammonia and 0.37 ± 0.04 eV molecule$^{-1}$ for methylamine in ices without isotopic labeling. A penetration depth of 348 ± 10 nm was determined for ices without isotopic labeling with the aid of Monte Carlo simulations conducted with CASINO 2.42 (51) using parameters detailed in *SI Appendix*, Table S4. For the purposes of the simulation, the average density of the ice components, 0.680 g cm$^{-3}$ at 18 K for ammonia and 0.732 g cm$^{-3}$ for methylamine at 18 K, was used as an approximation for the unknown density of the mixed ices (49). Variations in density due to isotopic labeling were taken into account. The average penetration depth (288 to 358 nm, *SI Appendix*, Table S4) is significantly less than the ice thickness (730 ± 30 nm) by design to prevent energetic electron initiated interactions between the ice and the silver substrate. Energetic doses reported in *SI Appendix*, Table S3 represent the calculated total absorbed dose averaged over all molecules between the ice surface and the average penetration depth. FTIR spectra were measured before, during, and after irradiation to verify changes in the spectrum due to reactions and to determine new functional groups and smaller species produced.

Photoionization reflectron time-of-flight mass spectrometry (PI-ReToF-MS) utilized in this research has been discussed in detail previously (44). Ices were heated to 320 K with TPD at a rate of 1 K min$^{-1}$. During TPD, pulsed 30 Hz coherent VUV light was passed 2 mm above the surface of the ice to photoionize subliming molecules. VUV light was produced via several resonant four-wave mixing ($\omega_{VUV} = 2\omega_1 \pm \omega_2$) schemes detailed in *SI Appendix*, Table S5. After generation of the selected $\omega_1$ and $\omega_2$, the lasers were made collinear and focused (Thorlabs, LA5479, $f$ = 300 mm) into a jet of rare gas in the VUV generation vacuum chamber. Coherent VUV light exiting this chamber was separated from $\omega_1$ and $\omega_2$ by passing the collinear beams through an off-axis lithium fluoride (LiF) biconvex lens (Korth Kristalle, $R_1 = R_2 = 131.22$ mm) which collimates the light, imparts an angular separation between the three wavelengths, and directs the VUV light through an aperture to the ionization region. VUV intensity is measured by a Faraday cup on the opposite side of the ionization region, and ion counts were corrected for variations in VUV power based on the average power recorded during each mass spectrum accumulation. Ions formed are mass-analyzed in a reflectron time-of-flight mass spectrometer (ReToF-MS; Jordan TOF Products) and detected with a microchannel plate (MCP) detector (Jordan TOF Products). MCP signal was amplified (Ortec, 9305) before discrimination and amplification to 4 V (Advanced Research Instruments Corp., F100-TD) and recorded by a multichannel scaler (FAST ComTec, MCS6A) interfaced to a personal computer. Ion arrival times were recorded to 3.2 ns accuracy, mass spectra were repeated at a rate of 30 Hz, and new mass spectra were accumulated every 2 minutes during TPD until the temperature of the sample reached 320 K.

**Computational.** The optimized geometries and harmonic zero-point vibrational energies (ZPVEs) are determined with coupled cluster theory at the singles, doubles, and perturbative triples level [CCSD(T)] (52) along with the aug-cc-pVTZ basis set (53). The CCSD(T)/aug-cc-pVQZ single point energies at these same geometries are then extrapolated to the complete basis set limit via a two-point formula (54). The closed-shell neutral molecules employ restricted Hartree–Fock reference wavefunctions, while the open-shell doublet radical cations employ restricted open-shell Hartree–Fock references. The relative energies are computed as adiabatic differences between the energies plus corresponding ZPVEs of the optimized neutrals and the $C_{2v}$ $CH_2(NH_2)_2$ energy + ZPVE. The adiabatic ionization potentials are computed as the adiabatic energy + ZPVE differences between the neutrals and corresponding cations. All computations utilize the MOLPRO 2019.2 quantum chemistry program (55–57).

**Data, Materials, and Software Availability.** All study data are included in the article and/or *SI Appendix*.

**ACKNOWLEDGMENTS.** The experiments at the University of Hawaii were supported by the United States National Science Foundation Division for Astronomy (NSF-AST 2103269). The W. M. Keck Foundation and the University of Hawaii at Manoa financed the construction of the experimental setup. R.C.F. acknowledges support from NASA, grants NNX17AH15G & NNH22ZHA004C, start-up funds provided by the University of Mississippi, and computational support from the Mississippi Center for Supercomputing Research funded in part by NSF grants CHE-1338056 and OIA-1757220.

Author affiliations: [a]Department of Chemistry, University of Hawaii at Manoa, Honolulu, HI 96822; [b]W. M. Keck Research Laboratory in Astrochemistry, University of Hawaii at Manoa, Honolulu, HI 96822; and [c]Department of Chemistry & Biochemistry, University of Mississippi, MS 38677

1. J. M. Berg, J. L. Tymoczko, L. Stryer, *Biochemistry* (W. H, Freeman and Company, ed. 7, 2010).
2. D. E. Woon, The astrochymist (2022), https://www.astrochymist.org. Accessed 14 September, 2022.
3. F. A. Carey, R. A. Sundberg, *Advanced Organic Chemistry: Part A: Structure and Mechanisms* (Springer, New York, ed. 5, 2007).
4. F. A. Carey, R. A. Sundberg, *Advanced Organic Chemistry: Part B: Reactions and Synthesis* (Springer, New York, ed. 5, 2007).
5. A. Belloche *et al.*, Re-exploring molecular complexity with ALMA (ReMoCA): Interstellar detection of urea. *Astron. Astrophys.* **628**, A10 (2019).
6. A. J. Remijan *et al.*, Observational results of a multi-telescope campaign in search of interstellar urea [$(NH_2)_2CO$]. *Astrophys. J.* **783**, 77 (2014).
7. B. A. McGuire *et al.*, Interstellar carbodiimide (HNCNH): A new astronomical detection from the GBT PRIMOS survey via maser emission features. *Astrophys. J.* **758**, L33 (2012).
8. F. H. Crick, The origin of the genetic code. *J. Mol. Biol.* **38**, 367–379 (1968).
9. L. E. Orgel, Evolution of the genetic apparatus. *J. Mol. Biol.* **38**, 381–393 (1968).
10. L. E. Orgel, Prebiotic chemistry and the origin of the RNA world. *Crit. Rev. Biochem. Mol. Biol.* **39**, 99–123 (2004).
11. A. S. Menon, D. J. Henry, T. Bally, L. Radom, Effect of substituents on the stabilities of multiply-substituted carbon-centered radicals. *Org. Biomol. Chem.* **9**, 3636–3657 (2011).
12. L. Carballeira, I. Pérez-Juste, Ab initio study and NBO interpretation of the anomeric effect in $CH_2(XH_2)_2$ (X = N, P, As) compounds. *J. Phys. Chem. A* **104**, 9362–9369 (2000).
13. C. Wang, Z. Chen, W. Wu, Y. Mo, How the generalized anomeric effect influences the conformational preference. *Chem. Eur. J.* **19**, 1436–1444 (2013).
14. A. Vila, L. Estevez, R. A. Mosquera, Influence of the solvent on the charge distribution of anomeric compounds. *J. Phys. Chem. A* **115**, 1964–1970 (2011).
15. K. Eskandari, A. Vila, R. A. Mosquera, Interpretation of anomeric effect in the N-C-N unit with the quantum theory of atoms in molecules. *J. Phys. Chem. A* **111**, 8491–8499 (2007).
16. L. Carballeira, I. Pérez-Juste, Role of the anomeric effect in methanediamines in the gas phase and aqueous solutions. *J. Comput. Chem.* **22**, 135–150 (2001).
17. G. Leroy, J. P. Dewispelaere, H. Benkadour, D. R. Temsamani, C. Wilante, Theoretical approach to the thermochemistry of geminal interactions in $XY_2Hn$ compounds (X = C, N, O, Si, P, S; Y = $NH_2$, OH, F, $SiH_3$, $PH_2$, SH). The generalized anomeric effect re-examined. *Comput. Theor. Chem.* **334**, 137–143 (1995).
18. Y. P. Chang, T. M. Su, Global conformational analysis and the anomeric interactions of methanediol, methanediamine and aminomethanol. *Comput. Theor. Chem.* **365**, 183–200 (1996).
19. Y. P. Chang, T. M. Su, Intramolecular hydrogen bonding and anomeric interactions in $H_nXCH_2YH_m$ ($XH_n$, $YH_m$ = OH, $NH_2$, SH, $PH_2$): A global conformational analysis. *J. Phys. Chem. A* **103**, 8706–8715 (1999).
20. J. S. Wright, H. Shadnia, L. L. Chepelev, Stability of carbon-centered radicals: Effect of functional groups on the energetics of addition of molecular oxygen. *J. Comput. Chem.* **30**, 1016–1026 (2009).
21. D. Kaur, R. P. Kaur, R. Kohli, Substituent effect on N-H bond dissociation enthalpies of amines and amides: A theoretical study. *Int. J. Quant. Chem.* **109**, 559–568 (2009).
22. A. Nemirowski, P. R. Schreiner, Electronic stabilization of ground state triplet carbenes. *J. Org. Chem.* **72**, 9533–9540 (2007).
23. K.-S. Song, L. Liu, Q.-X. Guo, Effects of geminal disubstitution on C-H and N–H bond dissociation energies. *Tetrahedron* **60**, 9909–9923 (2004).
24. E. Gras, S. Chassaing, "Carbenes and nitrenes" in Organic Reaction Mechanisms · 2015: An Annual Survey Covering the Literature Dated January to December 2015, pp. 219–249 (2019).
25. P. Knudsen, Über methylendiamin. *Ber. Dtsch. Chem. Ges.* **47**, 2698–2701 (1914).
26. G. Galaverna, R. Corradini, A. Dossena, R. Marchelli, Diaminomethane dihydrochloride, a novel reagent for the synthesis of primary amides of amino acids and peptides from active esters. *Int. J. Pept. Protein Res.* **42**, 53–57 (1993).
27. H. Hettegger, A. Hofinger, T. Rosenau, Strain-induced reactivity effects in the reaction of 2,5-dihydroxy-[1,4]-benzoquinone with Diamines. *Curr. Org. Chem.* **25**, 529–538 (2021).
28. K. Nagaraj, S. Ambika, S. Rajasri, S. Sakthinathan, S. Arunachalam, Synthesis, micellization behavior, antimicrobial and intercalative DNA binding of some novel surfactant copper(II) complexes containing codified phenanthroline ligands. *Colloids Surf. B* **122**, 151–157 (2014).

Downloaded from https://www.pnas.org by University of Hawaii at Manoa Library on December 12, 2022 from IP address 128.171.57.189.

29. V. K. Gupta, M. Al Khayat, A. K. Singh, M. K. Pal, Nano level detection of Cd(II) using poly(vinyl chloride) based membranes of Schiff bases. *Anal. Chim. Acta.* **634**, 36–43 (2009).
30. J. W. ApSimon, R. W. Thompson, J. C. S. Wong, W. G. Craig, Some diazaspiranes from the reaction of ketones with ethylenediamine and 1,3-diaminopropane. *Heterocycles* **9**, 23–27 (1978).
31. V. Vinogradoff *et al.*, Acetaldehyde solid state reactivity at low temperature: Formation of the acetaldehyde ammonia trimer. *J. Phys. Chem. A* **116**, 2225–2233 (2012).
32. P. Theule *et al.*, Thermal reactions in interstellar ice: A step towards molecular complexity in the interstellar medium. *Adv. Space Res.* **52**, 1567–1579 (2013).
33. M. Meot-Ner, S. F. Nelsen, M. F. Willi, T. B. Frigo, Special effects of an unusually large neutral to radical cation geometry change. Adiabatic ionization energies and proton affinities of alkylhydrazines. *J. Am. Chem. Soc.* **106**, 7384–7389 (1984).
34. A. M. Turner, S. Chandra, R. C. Fortenberry, R. I. Kaiser, A photoionization reflectron time-of-flight mass spectrometric study on the detection of ethynamine ($HCCNH_2$) and 2H-azirine (*c*-$H_2CCHN$). *Chem. Phys. Chem.* **22**, 985–994 (2021).
35. C.-H. Chen, *Deuterium Oxide and Deuteration in Biosciences* (Springer, 2022).
36. C. Zhu *et al.*, A vacuum ultraviolet photoionization study on the formation of methanimine ($CH_2NH$) and ethylenediamine ($NH_2CH_2CH_2NH_2$) in low temperature interstellar model ices exposed to ionizing radiation. *Phys. Chem. Chem. Phys.* **21**, 1952–1962 (2019).
37. C. Zhu *et al.*, Synthesis of methanediol [$CH_2(OH)_2$]: The simplest geminal diol. *Proc. Natl. Acad. Sci. U.S.A.* **119**, e2111938119 (2022).
38. S. K. Singh, C. Zhu, J. La Jeunesse, R. C. Fortenberry, R. I. Kaiser, Experimental identification of aminomethanol ($NH_2CH_2OH$)-The key intermediate in the strecker synthesis. *Nat. Commun.* **13**, 375 (2022).
39. S. Bottinelli *et al.*, The c2d *Spitzer* spectroscopic survey of ices around low-mass young stellar objects. IV. $NH_3$ and $CH_3OH$. *Astrophys. J.* **718**, 1100–1117 (2010).
40. A. Nummelin *et al.*, A three-position spectral line survey of Sagittarius B2 between 218 and 263 GHz. II. data analysis. *Astrophys. J. Suppl. Ser.* **128**, 213–243 (2000).
41. B. E. Turner, A molecular line survey of Sagittarius B2 and Orion-KL from 70 to 115 GHz. II – analysis of the data. *Astrophys. J. Suppl. Ser.* **76**, 617–684 (1991).
42. M. Förstel, A. Bergantini, P. Maksyutenko, S. Góbi, R. I. Kaiser, Formation of methylamine and ethylamine in extraterrestrial ices and their role as fundamental building blocks of proteinogenic α-amino acids. *Astrophys. J.* **845**, 83 (2017).
43. Karin I. Öberg *et al.*, The c2d *Spitzer* spectroscopic survey of ices around low-mass young stellar objects. III. $CH_4$. *Astrophys. J.* **678**, 1032–1041 (2008).
44. M. J. Abplanalp, M. Förstel, R. I. Kaiser, Exploiting single photon vacuum ultraviolet photoionization to unravel the synthesis of complex organic molecules in interstellar ices. *Chem. Phys. Lett.* **644**, 79–98 (2016).
45. M. J. Abplanalp *et al.*, A study of interstellar aldehydes and enols as tracers of a cosmic ray-driven nonequilibrium synthesis of complex organic molecules. *Proc. Natl. Acad. Sci. U.S.A.* **113**, 7727–7732 (2016).
46. B. M. Jones, R. I. Kaiser, Application of reflectron time-of-flight mass spectroscopy in the analysis of astrophysically relevant ices exposed to ionization radiation: Methane ($CH_4$) and $D_4$-methane ($CD_4$) as a case study. *J. Phys. Chem. Lett.* **4**, 1965–1971 (2013).
47. R. I. Kaiser, S. Maity, B. M. Jones, Infrared and reflectron time-of-flight mass spectroscopic analysis of methane ($CH_4$)–carbon monoxide (CO) ices exposed to ionization radiation – Toward the formation of carbonyl-bearing molecules in extraterrestrial ices. *Phys. Chem. Chem. Phys.* **16**, 3399–3424 (2014).
48. A. M. Turner *et al.*, A photoionization mass spectroscopic study on the formation of phosphanes in low temperature phosphine ices. *Phys. Chem. Chem. Phys.* **17**, 27281–27291 (2015).
49. R. L. Hudson, Y. Y. Yarnall, P. A. Gerakines, Infrared spectral intensities of amine ices, precursors to amino acids. *Astrobiol.* **22**, 452–461 (2022).
50. M. Bouilloud *et al.*, Bibliographic review and new measurements of the infrared band strengths of pure molecules at 25 K: $H_2O$, $CO_2$, CO, $CH_4$, $NH_3$, $CH_3OH$, HCOOH and $H_2CO$. *Mon. Not. R. Astron. Soc.* **451**, 2145–2160 (2015).
51. D. Drouin *et al.*, CASINO V2.42–A fast and easy-to-use modeling tool for scanning electron microscopy and microanalysis users. *Scanning* **29**, 92–101 (2007).
52. K. Raghavachari, G. W. Trucks, J. A. Pople, M. Head-Gordon, A fifth-order perturbation comparison of electron correlation theories. *Chem. Phys. Lett.* **157**, 479–483 (1989).
53. T. H. Dunning, Gaussian basis sets for use in correlated molecular calculations. I. The atoms boron through neon and hydrogen. *J. Chem. Phys.* **90**, 1007–1023 (1989).
54. J. M. L. Martin, T. J. Lee, The atomization energy and proton affinity of $NH_3$. An ab initio calibration study. *Chem. Phys. Lett.* **258**, 136–143 (1996).
55. H.-J. Werner, P. J. Knowles, G. Knizia, F. R. Manby, M. Schütz, Molpro: A general-purpose quantum chemistry program package. *Wiley Interdiscip. Rev. Comput. Mol. Sci.* **2**, 242–253 (2012).
56. H. J. Werner *et al.*, The Molpro quantum chemistry package. *J. Chem. Phys.* **152**, 144107. (2020).
57. H.-J. Werner *et al.*, MOLPRO, 2019.2, A Package of Ab Initio Programs (2019). Accessed October 25, 2019.


Downloaded from https://www.pnas.org by University of Hawaii at Manoa Library on December 12, 2022 from IP address 128.171.57.189.